

This article was downloaded by: [UALR Ottenheimer], [Omar Abdulrazzaq]

On: 26 July 2013, At: 08:58

Publisher: Taylor & Francis

Informa Ltd Registered in England and Wales Registered Number: 1072954 Registered office: Mortimer House, 37-41 Mortimer Street, London W1T 3JH, UK



Particulate Science and Technology: An International Journal

Publication details, including instructions for authors and subscription information:

<http://www.tandfonline.com/loi/upst20>

Organic Solar Cells: A Review of Materials, Limitations, and Possibilities for Improvement

Omar A. Abdulrazzaq^a, Viney Saini^a, Shawn Bourdo^a, Enkeleda Dervishi^a & Alexandru S. Biris^a

^a Center for Integrative Nanotechnology Sciences, University of Arkansas at Little Rock, Little Rock, Arkansas, USA

Accepted author version posted online: 25 Feb 2013. Published online: 25 Jul 2013.

To cite this article: Omar A. Abdulrazzaq, Viney Saini, Shawn Bourdo, Enkeleda Dervishi & Alexandru S. Biris (2013) Organic Solar Cells: A Review of Materials, Limitations, and Possibilities for Improvement, Particulate Science and Technology: An International Journal, 31:5, 427-442, DOI: [10.1080/02726351.2013.769470](https://doi.org/10.1080/02726351.2013.769470)

To link to this article: <http://dx.doi.org/10.1080/02726351.2013.769470>

PLEASE SCROLL DOWN FOR ARTICLE

Taylor & Francis makes every effort to ensure the accuracy of all the information (the "Content") contained in the publications on our platform. However, Taylor & Francis, our agents, and our licensors make no representations or warranties whatsoever as to the accuracy, completeness, or suitability for any purpose of the Content. Any opinions and views expressed in this publication are the opinions and views of the authors, and are not the views of or endorsed by Taylor & Francis. The accuracy of the Content should not be relied upon and should be independently verified with primary sources of information. Taylor and Francis shall not be liable for any losses, actions, claims, proceedings, demands, costs, expenses, damages, and other liabilities whatsoever or howsoever caused arising directly or indirectly in connection with, in relation to or arising out of the use of the Content.

This article may be used for research, teaching, and private study purposes. Any substantial or systematic reproduction, redistribution, reselling, loan, sub-licensing, systematic supply, or distribution in any form to anyone is expressly forbidden. Terms & Conditions of access and use can be found at <http://www.tandfonline.com/page/terms-and-conditions>

REVIEW ARTICLE

Organic Solar Cells: A Review of Materials, Limitations, and Possibilities for Improvement

OMAR A. ABDULRAZZAQ, VINEY SAINI, SHAWN BOURDO, ENKELEDA DERVISHI, and
ALEXANDRU S. BIRIS

Center for Integrative Nanotechnology Sciences, University of Arkansas at Little Rock, Little Rock, Arkansas, USA

Significant attention has been given during the last few years to overcome technological and material barriers in order to develop organic photovoltaic devices (OPVs) with comparable cost efficiency similar to the inorganic photovoltaics (PVs) and to make them commercially viable. To take advantage of the low cost for such devices, major improvements are necessary which include: an efficiency of around 10%, high stability from degradation under real-world conditions, novel optically active materials, and development of novel fabrication approaches. In order to meet such stringent requirements, the research and development in OPVs need to improve upon the short diffusion length of excitons, which is one of the factors that are responsible for their low power conversion efficiency. This review discusses some of the most significant technological developments that were presented in the literature and helped improve photovoltaic performance, such as tandem architectures, plasmonics, and use of graphitic nanostructural materials, among others.

Tandem organic solar cells with embedded plasmonics are a promising approach to further increase the power conversion efficiency of organic solar cells, by harvesting complementary spectral regions with high quantum efficiencies. Polymeric nanocomposites incorporating graphitic nanostructures were extensively investigated for the next generation of efficient and low-cost solar cells, since such nanomaterials show excellent electrical and mechanical properties, excellent carrier transport capabilities, and provide an efficient pathway to the dissociated charge carriers.

Keywords: Carbon nanotubes, organic solar cells, plasmonics, tandem solar cells

1. Introduction

Photovoltaics are devices focused on converting light energy into electrical energy. In recent years, the growing demand for clean energy resources has led to a dramatic growth in the research, development, and manufacturing of solar cells. Inorganic solar cells, such as conventional silicon solar cells and heterojunction solar cells, are relatively mature technologies, and the power conversion efficiency of these devices is approaching record limits of about 24.7% for crystalline silicon solar cells (Zhao et al. 2001) and greater than 42.3% for certain multijunction solar cells (“Spire pushes solar cell record to 42.3%” 2010) exposed to more than 400 suns. Unless otherwise stated, all of the efficiencies mentioned in this article have been determined under AM1.5 illumination conditions.

Silicon-based devices have been the front runners in bringing solar cell technology to the consumer market (Tao 2008). However, fabrication processes are complex and involve a number of steps that make solar panels expensive and the energy they produce uncompetitive compared to traditional energy sources (e.g., coal, natural gas, hydropower, etc.). Moreover, silicon solar cells are rigid and cannot be industrially fabricated in large sizes due to the limitation of the silicon wafer processing technology.

These disadvantages of silicon PVs and their relative limited ability to provide cost-effective energy are some of the reasons that have led many researchers to explore alternative materials for solar energy generation. Some of the most promising materials are conjugated organic moieties. Organic photovoltaic cells are based on thin film polymers, small molecules, or both fabricated by very simple and cost-efficient techniques, such as spin coating, spray deposition, and printing. The inherent properties of OPV systems (Tang 1986) allow them to be used in applications requiring flexible and large area PV cells (Halls et al. 1995; G. Yu et al. 1995). Figure 1 highlights the mechanical flexibility of organic cells that facilitates their usage in a multitude of shapes and applications.

Present address for E. Dervishi: Center for Integrated Nanotechnologies, Materials Physics and Application Division, Los Alamos National Laboratory, Los Alamos, New Mexico, USA.

Address correspondence to: Omar A. Abdulrazzaq and Alexandru S. Biris, Center for Integrative Nanotechnology Sciences, University of Arkansas at Little Rock, Little Rock, AR 72204, USA. E-mail: oaabdulrazza@ualr.edu, asbiris@ualr.edu



Fig. 1. Organic cells are flexible enough to be bent and/or rolled. Image reproduced from Brabec and Durrant (2008) with kind permission from Cambridge University Press. (Figure available in color online.)

Although OPVs have a low cost and are easy to fabricate and mechanically suitable, this new generation PV system is still under technological development. OPVs are usually categorized into small-molecule solar cells and polymer solar cells. In spite of the fact that polymer solar cells have achieved better conversion efficiency than small-molecule solar cells (Kietzke 2007), until recently small-molecule solar cells are reported to attain comparable efficiencies to polymer solar cells as a result of rapid improvements (Sun et al. 2012). The theoretical limit of the power conversion efficiency for organic thin film solar cells is lower than that of inorganic solar cells. According to Solarmer Energy Inc. (2009), a 10% power conversion efficiency is required for the commercialization of OPVs, and 15% power conversion efficiency is the highest expected result. Thus, OPVs cannot compete with inorganic solar cells in terms of power conversion efficiency, but they can become competitive in relation to the cost, fabrication simplicity, and novel applications (Kalowekamo and Baker 2009). In this review, the progress of organic solar cells along with efforts to develop high-efficiency devices and low-cost organic solar panels will be extensively discussed. Novel PV architectures, such as tandem cells, plasmon-enhanced cells, and the use of carbon nanomaterials with organic materials, are the primary focus of this review.

2. Solar Cells and Their Characteristics

The most important parameters that are widely used to determine the performance of solar cells are open-circuit voltage (V_{OC}), short-circuit current (I_{SC}), fill factor (FF), and power conversion efficiency (PCE). Figure 2 shows the typical current-voltage characteristics of a solar cell in dark and illuminated conditions. Short-circuit current is defined as the current produced by solar cells under illumination without application of any external potential. Open circuit voltage is the potential difference between two terminals of solar cells under illumination when there is no current flowing through the terminals. Fill factor is defined by the quotient of maximum power (P_M) generated by the solar cell and product of open-circuit voltage and short-circuit current.

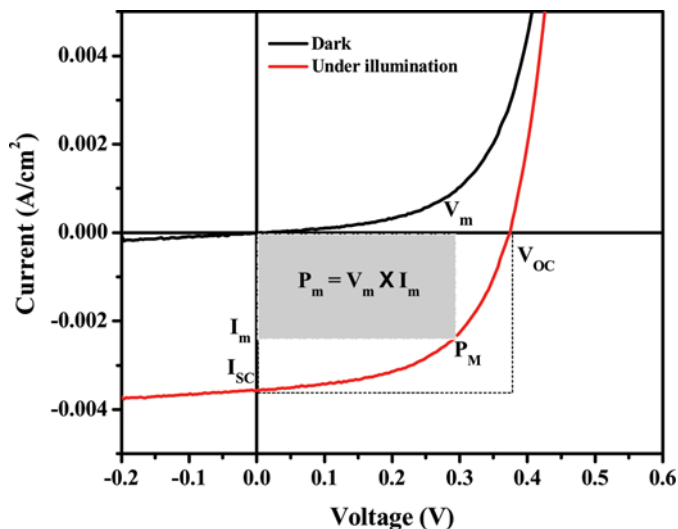


Fig. 2. Typical current-voltage response of a solar cell. (Figure available in color online.)

The power conversion efficiency, more commonly known as the efficiency of a solar cell, is the ratio of the maximum power generated by the solar cell to the incident radiant energy.

Some other important parameters in solar cell design and characterization are spectral responsivity (R_s) and quantum efficiency (QE). Spectral responsivity is defined as the quotient of the current coming out of the cell and the incoming light beam of a given power and wavelength. Quantum efficiency is determined by the number of electron-hole pairs collected per incident photon.

3. Construction of OPV Devices

An organic photovoltaic device is essentially comprised of at least four layers in addition to the transparent substrate as shown in Figure 3. The substrate, through which the device is to be illuminated, can be composed of glass, polyester, or

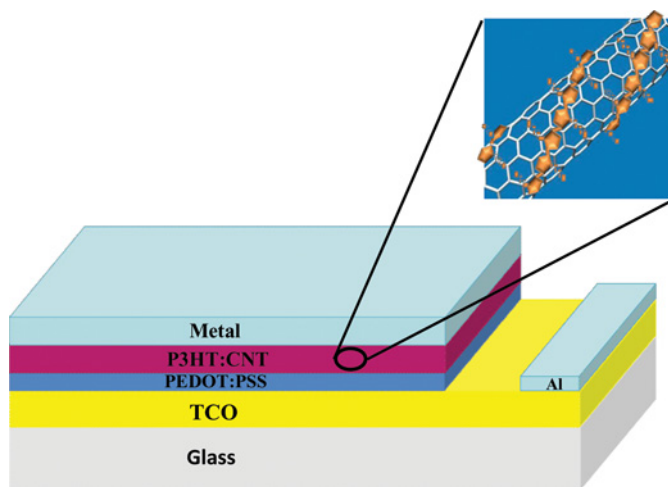


Fig. 3. A schematic diagram for a typical basic organic cell with CNTs as an acceptor within the active layer. (Figure available in color online.)

many other transparent materials. Sometimes a stainless steel substrate is used, but, in this case, the substrate is designed as the backside of the cell (Galagan et al. 2012). The superstrate material could be coated with a transparent conductive oxide (TCO), such as indium tin oxide (ITO); generally, both glass and polyethyleneterephthalate (PET) pre-coated with ITO are commercially available. Recent reports have suggested that carbon nanotubes (CNTs) can be used as the transparent conductive layer instead of transparent conductive oxides (Rowell et al. 2006). The transparent layer has a dual purpose: it acts as a transparent window layer and as an anode to collect the photogenerated holes. It has been reported that the elements of the anode may diffuse into the active layer and cause device degradation due to the formation of charge trap centers (Jing et al. 2005). To prevent this problem, a protective layer is placed between the active layer and the anode; poly(3,4-ethylenedioxythiophene) poly(styrenesulfonate) (PEDOT:PSS) is the best option available, thus far. PEDOT:PSS acts as an electron-blocking layer, in addition to assisting in the efficient transportation of photogenerated holes to the anode. Also, PEDOT:PSS serves to smooth out the surface roughness of the ITO (Edwards 2007). The electron-blocking hole-transport layer (HTL) is essential in bulk heterojunction devices rather than bilayer devices. This is because in bulk devices, without an HTL, both the donor and acceptor touch the anode and the cathode resulting in the flow of electrons and holes to the same electrode and causing poor device performance. Polyaniline doped with camphorsulfonic acid has also been used as a hole transport layer. It has been found that protonation level of polyaniline can play an important role on the performance of the HTL (Abdulrazzaq et al. 2013). The active layer consists of donor and acceptor organic materials, either applied in layer-by-layer geometry (planar or bilayer heterojunction) or mixed together to create a blend (bulk heterojunction). Lately, CNTs have been used as acceptors instead of organic acceptors to create a nanocomposite active layer as will be discussed in detail later. Light passes through the transparent electrode then through the HTL and is absorbed in the active layer. The last layer is the cathode which is generally aluminum, copper, or another metal having a suitable work function that can achieve better electron transport. Some researchers have proposed LiF between the cathode and the active layer as a protective buffer layer to prevent diffusion of cathode elements to the active layer and also to act as an electron-transport, hole-blocking layer (Jing et al. 2005). The main problem with using some of these buffer layers is the high deposition temperature that can potentially damage the active layer underneath. Further studies related to the stability of the organic layers and degradation due to the diffusion of cathode elements into the active layer can be found in the literature (Jorgensen et al. 2008).

4. Carrier Transport Mechanism in the OPV

The three phenomena that occur during the operation of a solar cell are as follows: i) light absorption to generate electric charge carriers, ii) charge separation, and iii) charge transport to electrodes. The light is absorbed by a photoactive layer generating either free charge carriers (traditional inorganic

PV devices) or excitons (OPV devices) upon photoexcitation. The charge carriers are collected and separated by the formation of a p-n junction between two semiconducting materials (traditional inorganic PV devices) or a donor-acceptor interface (organic PV devices). Finally, the charges are swept away by metal electrodes to the outer circuitry.

The mechanism of photocurrent generation in p-n junction solar cells is well-known and has been proven both theoretically and experimentally since the 1950s when the first efficient silicon p-n junction solar cell was developed at Bell laboratories (Chapin et al. 1954). Extensive investigations on Schottky metal-semiconductor (MS) solar cells, as well as metal-insulator-semiconductor (MIS) and metal-oxide-semiconductor (MOS) solar cells, have been performed (Nielsen 1980). Multijunction solar cells based on three cells (separated by two buffer layers) are the best known solar cells because they exhibit the highest conversion efficiency to date ("Spire pushes solar cell record to 42.3%" 2010). A typical example of these complex solar cells is the Ge/InGaP/InGaAs/AlGaInP/AlInP/GaAs multijunction solar cell. In conventional inorganic homojunction and heterojunction solar cells, the difference in charge carrier concentration between two intimately contacted semiconductors results in diffusion of charges from regions of higher to lower concentration. Under equilibrium conditions, a built-in potential (V_{bi}) and an internal electric field are created. The photogenerated current resulting from absorption of an incident photon causes an electronic transition from the valence band to the conduction band. This transition occurs if the photon energy is equal to or greater than the band gap of the material. Electrons in the conduction band and associated holes in the valence band are approximately free because of the continuous nature of the energy band levels. In addition, the Coulomb force between these pairs is very low, virtually lower than the thermal energy (kT/q). The internal electric field that arises from the built-in potential drives the photogenerated electrons into the cathode and the photogenerated holes into the anode. The accumulation of photogenerated carriers on the two electrodes creates an electromotive force at the outside circuit which is usually called V_{OC} . The V_{OC} in silicon p-n junction solar cells is generally about 0.5 V and can be greater in other types of heterojunctions and Schottky junctions.

In organic devices, the light interaction with an OPV does not create free electron-hole pairs; instead, the absorption of the photon creates a photoexcitation pair, a so-called exciton, that is bound by Coulomb attractions. In this case, the binding energy is larger than the thermal energy. The binding energy of the exciton in organics is around 0.25 eV (Barth and Bassler 1997), while that of thermal energy at room temperature is 0.025 eV, which is insufficient to dissociate the exciton. Under these circumstances, exciton dissociation requires a large internal electric field. Fortunately, the internal field in organic heterojunctions is intrinsically high, and the record V_{OC} of >0.7 V (Chen et al. 2009; Vandewal et al. 2009) is higher than that of conventional silicon p-n junction solar cells.

Organic solar cells are comprised of donor and acceptor moieties brought into intimate contact to form a

donor-acceptor heterostructure. When a photon of sufficient energy is absorbed in donor, the electron hops into the lowest unoccupied molecular orbital (LUMO), leaving a hole in the highest occupied molecular orbital (HOMO); hence, an exciton will be generated. The exciton recombines unless it is quickly dissociated. In order to dissociate the exciton, the acceptor material has to offset the binding energy of the exciton in the donor. The charge transfer at the interface can only take place when the following condition is satisfied:

$$E_A^A - E_A^D > U_D, \quad (1)$$

where E_A refers to electron affinity, and U_D is the binding energy of exciton in donor; the superscripts A and D stand for acceptor and donor, respectively. If the acceptor is chosen to have an electron affinity greater than that of the donor, the photogenerated electron in donor will transport to the LUMO of acceptor. If the HOMO of acceptor is lower than the HOMO of donor, the hole in donor does not transport to acceptor, and dissociation occurs as shown in Figure 4a. Otherwise, the whole exciton could transfer to the acceptor, and dissociation would not occur (Kietzke 2007) as shown in Figure 4b.

The probability of dissociation is increased if the potential difference ($\Delta\phi$) between the LUMO of donor and the LUMO of acceptor is increased. This case can be fulfilled by choosing two different organic semiconductors with large offset (ΔE) and, hence, large V_{bi} and consequently large V_{OC} (Fonash 1981). Theoretically, V_{bi} is given by (Scharber et al. 2006):

$$V_{bi} = E_{LUMO}(\text{acceptor}) - E_{HOMO}(\text{donor}), \quad (2)$$

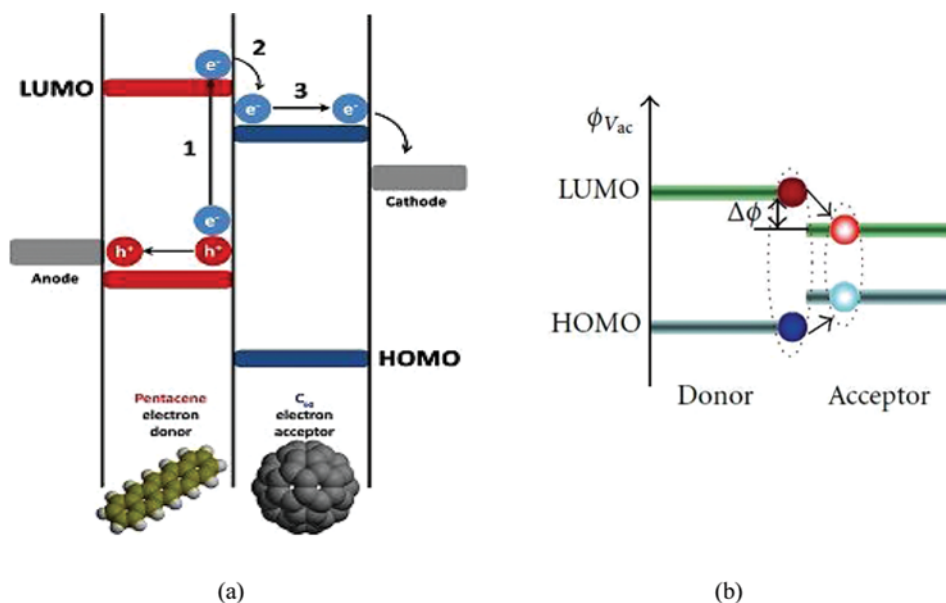


Fig. 4. a) Preferential staggered gap in which exciton dissociates, b) nonpreferential straddling gap in which the whole exciton is transferred from donor to acceptor, and dissociation does not occur (Kietzke 2007). Image in Figure 4a reproduced with permission of Alan Aspuru-Guzik and the Clean Energy Project (<http://cleanenergy.harvard.edu>, <http://aspuru.chem.harvard.edu>). Image B reproduced from Kietzke (2007). (Figure available in color online.)

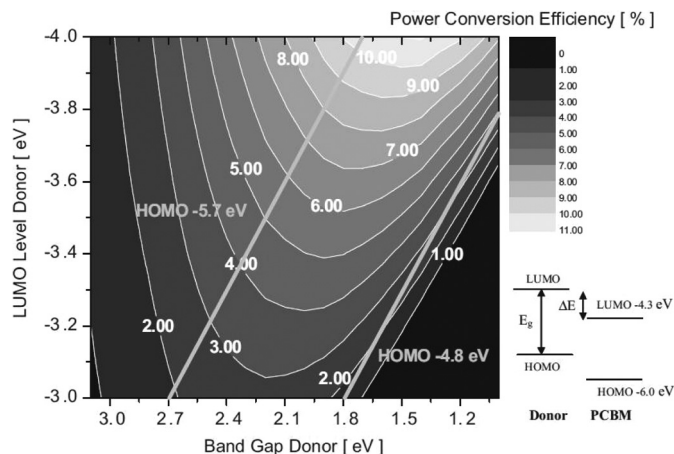


Fig. 5. Contour plot of the calculated PCE where the calculations are made by neglecting the absorption at the acceptor side Scharber et al. Design rules for donors in buck-heterojunction solar cells-towards 10% energy-conversion efficiency. *Advanced Materials* (2006) 18: 789–794. Copyright Wiley-VCH Verlag GmbH & Co. KGaA. Reproduced with permission.

while V_{OC} is empirically given by the following equation (Scharber et al. 2006):

$$V_{OC} = V_{bi} - 0.3. \quad (3)$$

The calculated PCE depends on both the LUMO offset and the bandgap of the donor material used. Figure 5 shows a contour plot for the calculated efficiency as a function of

the LUMO and bandgap of a donor at a specific LUMO and bandgap of an acceptor (namely LUMO = -4.3 eV and bandgap = 1.7 eV) and constant donor HOMO levels of -5.7 and -4.8 eV (Scharber et al. 2006).

5. Limitations of Photocurrent in OPV

Although OPVs show acceptable PCEs, the technology has not yet been widely commercialized. Most of the published results have reported $\sim 5.5\%$ PCE for bulk heterojunction cells (Peet et al. 2007) and slightly more than 6% PCE (under 2 suns) for tandem devices (J. Kim et al. 2007). However, significant strides have been made in the last three years to introduce devices with more than 7% PCE (Liang et al. 2010) and lately above 8% . There have been two NREL certified devices that have broken the 8% PCE mark; the Solarmer Company (2009) has achieved a device exhibiting 8.13% PCE, and Yang's group has announced an 8.6% PCE (Dou et al. 2012) that is the highest certified PCE for organic solar cells to date up to our best knowledge.

Various advancements in OPV technologies have been made to increase the PCE. The V_{OC} of such devices is easily heightened by choosing a large ΔE between the D_{LUMO} and A_{LUMO} . Choosing a large ΔE to efficiently dissociate the excitons is not in and of itself challenging, but getting the dissociated carriers to the electrodes is difficult due to several parameters that affect the amount of photocurrent reaching the outside circuitry. In fact, the mobility and diffusion length of charge carriers in organic semiconductors are very small when compared with those of inorganic semiconductors, and this is the biggest challenge that negatively affects the photocurrent in OPVs. For instance, the electron and hole mobilities of organic semiconductors are a hundred times lower than the electron and hole mobilities of single crystal silicon. The diffusion length of excitons in organic semiconductors ranges between 10 and 40 nm (on average) (Halls et al. 1996; Halls and Friend 1997; Kerp et al. 1998), while the diffusion length of electrons in monocrystalline silicon is on the order of micrometers (Nara and Sakaguchi 2003). The low value of diffusion length limits the ideal thickness of the organic layer to a few tens of nanometers (which is good from an economic standpoint), but efficient absorption of incident light requires a thickness of a few hundred nanometers. Luckily, the absorption of many organic materials is intrinsically high even for low thicknesses (Hoppe and Sariciftci 2004).

In order to overcome these shortcomings of OPVs, several approaches are considered when designing materials and devices: i) increase the electrical conductivity of organic materials by improving the crystal structure (Aziz et al. 2007), ii) create a large donor-acceptor interface to promote the dissociation of more excitons, and iii) collect a high number of photogenerated carriers. Crystalline organic materials exhibit better charge transport capabilities than amorphous organic materials. Since these films are processed from solution, the crystallinity can be improved by choosing appropriate solvents and by thermal annealing after deposition (Yin et al. 2007). A new study pointed out that applying an electric field during annealing may result in more than

25% improvement in PCE (Bagui and Iyer 2011) for some organic cells. Several studies have revealed that the slow evaporation of high boiling-point solvents improves organic material structure and results in OPVs with superior photovoltaic characteristics (Arias et al. 2001). Other studies have demonstrated that both crystallinity and photovoltaic performance can be affected by various annealing times and annealing temperatures (Hau et al. 2010).

6. OPV Device Architecture

A primitive organic solar cell is generally comprised of two intimately contacted donor and acceptor layers (the so-called bilayer OPV heterojunction also referred to as planar OPV heterojunction) (Tang 1986). In a bilayer heterojunction, acceptor and donor are brought into intimate contact by subsequent deposition of the two layers. The bilayers are sandwiched between two electrodes to achieve an ohmic contact to the acceptor and donor, respectively. The electrode located on the donor side, called the cathode, should be transparent with a high work function (ITO is one of the best choices) (Hashimoto and Hamagaki 2006). The other electrode (anode) with a low work function is deposited on the acceptor side. Light penetrates the heterojunction through the transparent cathode.

This architecture has failed to achieve high PCE because many generated excitons do not reach the interface (G. Yu et al. 1995). Only those excitons that have been generated near the junction ($< \sim 20$ nm) have the chance to dissociate. The excitons generated at greater distances from the junction ($> \sim 20$ nm) recombine before reaching the donor-acceptor interface due to the short diffusion length and low mobility. Figure 6 depicts schematically the exciton dissociation and/or exciton recombination in the bilayer organic heterojunction.

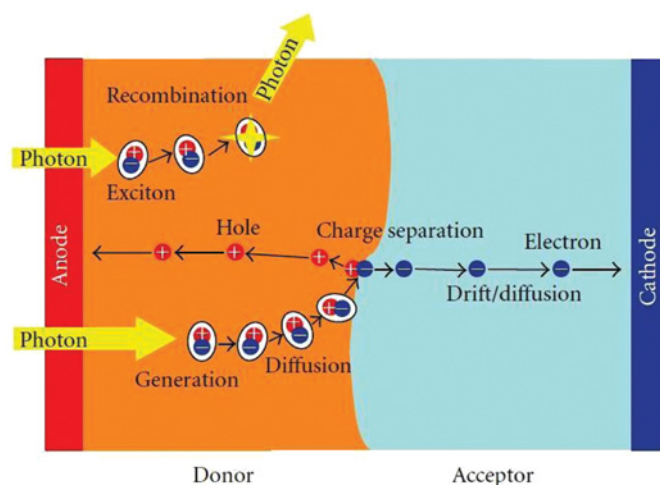


Fig. 6. Charge transfer in bilayer OPV heterojunction. Image produced from Kietzke (2007). (Figure available in color online.)

The improvement in photovoltaic performance of bilayer organic heterojunctions requires a diffusion length comparable to the dimensions of the bilayer junction. The diffusion length of organic semiconductors is very low, even for those demonstrating high conductivity; the transport process in organic materials is governed by hopping transport while in inorganic semiconductors the phenomenon is described by band transport (Kietzke 2007). Thus, solutions for significantly increasing diffusion length are continually being sought out. Since it is unclear how to increase the diffusion length of organic semiconductors, the thickness of the active layer can be decreased in such a way that it is comparable to the diffusion length of excitons. However, in ultra-thin layers, the low optical absorption significantly reduces the number of photogenerated excitons. Organic bilayer heterojunctions are less prevalent due to the advances made in the bulk heterojunction devices (Scharber et al. 2006). In bulk heterojunctions design, the junction interface is large due to the nanometer separation between donor and acceptor domains that allows for exciton formation and dissociation deep inside the bulk of active layer.

To fabricate bulk heterojunctions, the donor and acceptor organic semiconductors are mixed into a solution. The solution is deposited in the form of a thin film, and the phase separation between donor and acceptor occurs, which introduces nanojunctions inside the bulk. The photogenerated exciton has an increased probability of diffusion to a nearby interface and dissociate into an electron and hole. The bulk heterojunction concept, shown pictorially in Figure 7, has created broader interest in OPV research (G. Yu et al. 1995), and the PCEs obtained from this architecture are much higher than those obtained from bilayer heterojunctions (Peumans et al. 2003). Generally, both small-molecule and polymer solar cells attain the highest PCE from bulk heterojunction architecture.

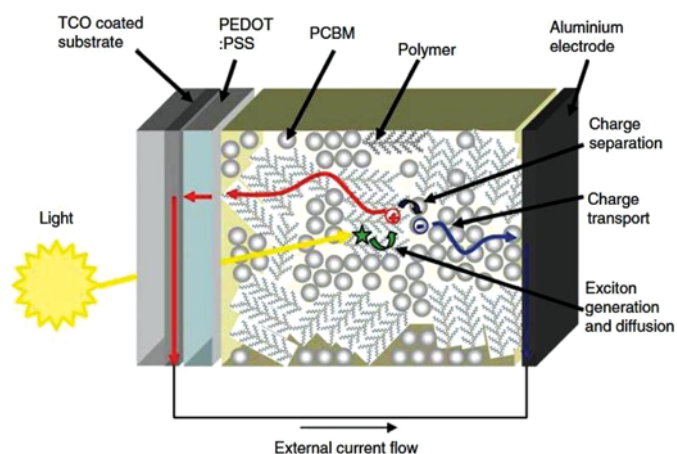


Fig. 7. Charge transfer in bulk OPV heterojunctions. Image reproduced from Brabec and Durrant (2008) with kind permission from Cambridge University Press. (Figure available in color online.)

7. Small-Molecule Heterojunction Solar Cells

The potential to use organic materials for solar cell technology was first observed in 1975 by Tang and Albrecht (Tang and Albrecht 1975), but the PCE was very low. This early prototype was a Schottky diode solar cell with chlorophyll-*a* as the semiconducting material. For almost a decade, little progress was made in the field; in 1986, further efforts by Tang were believed to be the first steps towards the realization of commercialized OPV technology (Tang 1986). This new device was based on a bilayer heterojunction OPV that consisted of copper phthalocyanine (CuPc) as the donor layer and 3,4,9,10-perylenetetracarboxylic-bis-benzimidazole (PTCBI) as the acceptor layer. A PCE of 1% was recorded, which represented a significant development. In 2003, Peumans et al. (2003) reported a 1.5% PCE for CuPc-PTCBI blend. Mutolo et al. (2006) reported an enhancement in the V_{OC} by increasing the band offset using a subphthalocyanine (SubPc)/buckminsterfullerene (C_{60}) bulk heterojunction. The PCE of this structure was 2.1%. A PCE of 3.8% was reported by Drechsel et al. (2005) using double p-i-n architecture, and Schulze et al. (2006) obtained a PCE of 3.4% using α,α' -bis(2,2-dicyanovinyl)-quinoxaline (DCV5T)/ C_{60} bulk heterojunction. Small-molecule solar cells did not pass the 5% power conversion efficiency in either bilayer or bulk architectures until 2012, when Sun et al. (2012) reported a breakthrough of 6.7% PCE. This bulk heterojunction device was comprised of small molecules: the donor material was 5,5'-bis{(4-(7-hexylthiophen-2-yl)thiophen-2-yl)-[1,2,5]thiadiazolo[3,4-c]pyridine}-3,3'-di-2-ethylhexylsilylene-2,2'-bithiophene, DTS (P TTh₂)₂ with PC₇₀BM as an acceptor.

8. Polymer Heterojunction Solar Cells

The unique properties of organic conducting polymers were first discovered by Heeger, Shirakawa, and MacDiarmid in the 1970s during work performed on polyacetylene. This discovery was the genesis of an enormous amount of work in the area of organic electronics and was finally honored with the Nobel Prize in Chemistry in 2000 (Heeger 2001). Conducting polymers, so-called synthetic metals, have an alternating backbone of sp^2 hybridized σ -bonds in addition to the unhybridized π -bond, which gives rise to the intrinsic conductive properties of these highly conjugated materials.

Polymer solar cells (sometimes called plastic solar cells) are preferable to small-molecule solar cells because of their facile processing techniques (Kietzke 2007). An ordered bulk heterojunction is easier to achieve in polymers than small molecules due to the low entropy of mixing. If two polymers are dissolved in the same solvent, phase separation occurs during solvent evaporation (Kietzke 2007). Another advantage of polymer-based OPVs is that the exciton dissociation is more effective than that for small molecules. In reality, the polymer-polymer blend is able to separate most of the photogenerated excitons if the fabrication conditions are optimized.

Bilayer polymer-polymer heterojunction solar cells do not exhibit high PCE because of the short diffusion length of the excitons. The best results for bilayer polymer-polymer solar

cells were reported by Alam and Jenekhe (2004) by using a poly(benzimidazobenzophenanthroline ladder) (BBL) and poly(1,4-phenylenevinylene) (PPV) bilayer solar cell. They reported a PCE of 4.6% under 1 mW/cm^2 illumination density; unfortunately, the efficiency of this device drops to 1.5% at AM1.5 illumination density.

In 1995, Halls et al. (1995) reported the first polymer-polymer bulk heterojunction. Their results were poor, but their work provided the foundation for a new generation of polymer devices. Afterward, much effort was devoted to the development of such devices. In 2005, a PCE of 1.7% was recognized by Kietzke et al. (2005) using a blend of (poly[2,5-dimethoxy-1,4-phenylene-1,2-ethynylene-2-methoxy-5-(2-ethylhexyloxy)-(1,4-phenylene-1,2-ethynylene)]) (M3EH-PPV) as the donor and (poly[oxa-1,4-phenylene-1,2-(1-cyano)ethynylene-2,5-dioctyloxy-1,4-phenylene-1,2-(2-cyano)ethynylene-1,4-phenylene]) (CN-PPV) as the acceptor. Annealing was added to the fabrication process to improve the PV characteristics.

Poly(3-hexylthiophene) (P3HT) donor-polymer and Phenyl- C_{61} -butyric acid methyl ester (PCBM) acceptor-small molecules are typically used in polymer-small molecule architecture. In such devices, P3HT serves as a narrow-bandgap donor and helps to improve the absorption in the long wavelength region while PCBM serves as a wide-bandgap acceptor and enhances absorption in the short wavelength region. PCBM is preferred over other small molecules due to the ease of use and its high solubility in chloroform, chlorobenzene, dichlorobenzene, and toluene, which are commonly used solvents for P3HT. An efficiency of 5% has been obtained from this architecture (Ma et al. 2005). New attempts are now devoted to introducing polymer-small-molecule solar cells from a variety of materials that can cover the maximum solar spectrum (Camaioni et al. 2005; Li et al. 2006; Muhlbacher et al. 2006; W. Shin et al. 2006; R. Shin et al. 2007; Xia et al. 2006; F. Zhang et al. 2006).

Although P3HT is one of the most widely used polymers in OPVs with PCBM, there are some novel polymers that are potential replacements for P3HT because their lower bandgap absorbs more light and their lower HOMO level increases the V_{OC} of the cell (Chen et al. 2009). Poly[4,8-bis-substituted-benzo[1,2-b:4,5-b']dithiophene-2,6-diyl-alt-4-substituted-thieno[3,4-b]thiophene-2,6-diyl] (PBDTTT) is one example of these promising materials. Another new polymer is 5,6-difluoro-4,7-dithien-2-yl-2,1,3-benzothiadiazole (DTfBT) and benzo[1,2-b:4,5-b']dithiophene (BnDT) as the donor with PCBM as the acceptor. Recent results showed 7.2% efficiency of these devices (Zhou et al. 2011).

9. Tandem Organic Solar Cells

The aforementioned organic solar cell architectures are limited in the spectral range they cover. Some organic cells absorb in the short wavelength region and others absorb in long wavelength region. To maximize the solar spectrum absorption one should design solar cell structure that can harness energy from as much of the solar spectrum as possible and more specifically within 400–900 nm wavelength range.

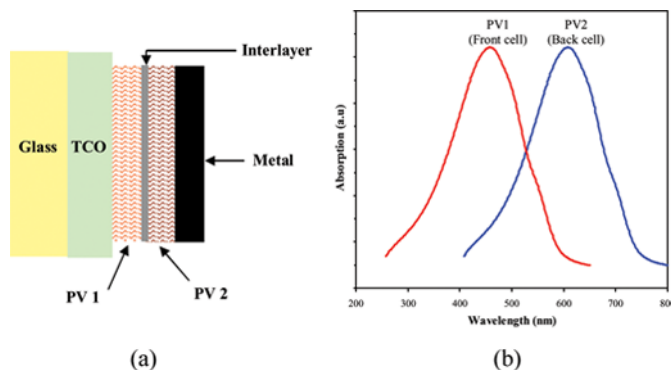


Fig. 8. a) Tandem organic solar cell: the front PV absorbs the shorter wavelengths while the back PV absorbs the longer wavelengths; b) absorption range of tandem solar cells. (Figure available in color online.)

A large portion of this wavelength range is best formed using a tandem architecture (Aziz et al. 2007) which is similar to that depicted in Figure 8a. Tandem organic solar cells are comprised of two subcells separated by an interlayer. It is possible to increase the absorption spectrum by adding more subcells in this type of architecture, but it adds to fabrication complexity and cost. Each subcell is engineered to operate in a different region of the solar spectrum. Figure 8b describes the concept behind the tandem cell, where the front cell (PV1) functions in the wavelength range of 300–600 nm and back cell (PV2) absorbs between 450 and 750 nm.

Initial attempts to create tandem cells failed to achieve the expected increase in PCE (Dennler et al. 2006) because they were based on multilayer fabrication technology, where the two subcells are stacked together without placing a buffer layer in between them. The maximum current that can be obtained from these multilayer devices is limited by the lowest current produced by any one of the subcells. Placing an interlayer between the two subcells helps to collect all of the photocurrent produced by each subcell. In the last few years, very encouraging results have been recorded for this architecture (Shrotriya et al. 2006). 6% PCE was reported by J. Kim et al. (2007) using a P3HT:PCBM subcell with poly[2-methoxy-5-(2'-ethyl-hexyloxy)-1,4-phenylene vinylene] (MEH-PPV):PCBM subcell and TiO_x as a buffer layer. Work on tandem devices has shown PCEs greater than 7% (Brabec et al. 2010), and more recently, an 8.6% PCE has been achieved by Yang's group (Dou et al. 2012) pushing OPVs closer to the 10% efficiency milestone.

10. Plasmonics in Organic Solar Cells

Since the exciton diffusion length in organic solar cells ranges between 10 and 40 nm, the active layer must be relatively ultra-thin; the thicknesses should be in the order of the absorption length of the materials used as the active layer. Therefore, the absorption efficiency will not be high enough, while considerably high PCE requires high absorption efficiency. To augment the absorption of incident light in active layer without increasing its thickness, plasmonic

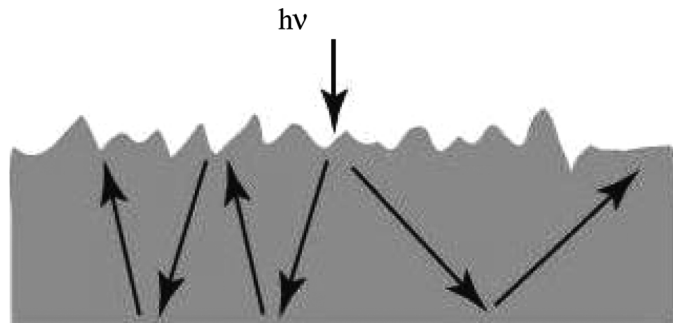


Fig. 9. Surface texturing of silicon wafer. Image reproduced from Yu et al. (2010) with permission from PNAS.

materials and structures can be exploited, which can trap the light inside the active layer. With the aid of this technique, the opportunity for photon absorption can be increased even for ultra-thin layers (Ferry et al. 2010).

The plasmonic phenomenon or light-trapping structure was first developed in 1981 by Goetzberger (Goetzberger et al. 1981). The initial work began on bulk silicon by texturing the silicon surface into a “roughened” pyramid-like structure (Atwater and Polman 2010) as shown in Figure 9.

Such a structure helps confining the light inside the bulk silicon. The refractive index of silicon is relatively high (~3.5) which makes the light scatter preferentially into the silicon side and concomitantly increases the optical path of light inside the silicon. This results in several folds increase in light absorption in a silicon wafer (Z. Yu et al. 2010). Surface texturing is not amenable to thin film technologies because the carrier generation in thin films occurs very close to the surface while the texturing acts as a trap for the photogenerated carriers (Catchpole and Polman 2008). Moreover, the surface roughness would exceed the film thickness; therefore, surface texturing is not an option in thin film solar cells. To increase the light absorption in thin film solar cells, three routes have been adopted: a) embedding nanoparticles on the surface of the solar cells, b) putting nanoparticles inside the active layer; and c) grating the back contact from the side of the active layer. These three examples of plasmonics are illustrated in Figure 10 and summarized in the following paragraphs.

In the first example (Figure 10a), small nanoparticles (preferably spheres less than 100 nm in diameter) are halfway

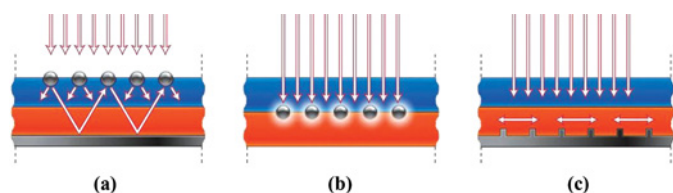


Fig. 10. Light trapping used in thin film solar cells. Reprinted by permission from Macmillan Publishers Ltd.: Atwater, H. A., and Polman, A. (2010). Plasmonics for improved photovoltaic devices. *Nature Materials* 9: 205–213. (Figure available in color online.)

embedded in the surface of the semiconductor. In cell structures harvesting wavelengths from 500 to 800 nm, light trapping of 85% has been obtained (Atwater and Polman 2010). In this design, light is scattered into the material with higher permittivity, which in this case is the thin film semiconductor because the other medium is air. Scattering leads to an increase in the optical path length of light inside the semiconductor thereby increasing overall absorption. The shape and size of the nanoparticles greatly affect the angular spread as seen in Figure 11. In a well-designed plasmonic solar cell, thickness can be decreased up to one hundred-fold while maintaining similar absorption characteristics (Atwater and Polman 2010).

The second example (Figure 10b) utilizing plasmonics is based on the fact that the dielectric difference between the host semiconductor and the implanted metallic nanoparticles is significantly higher, resulting in a plasmon mode

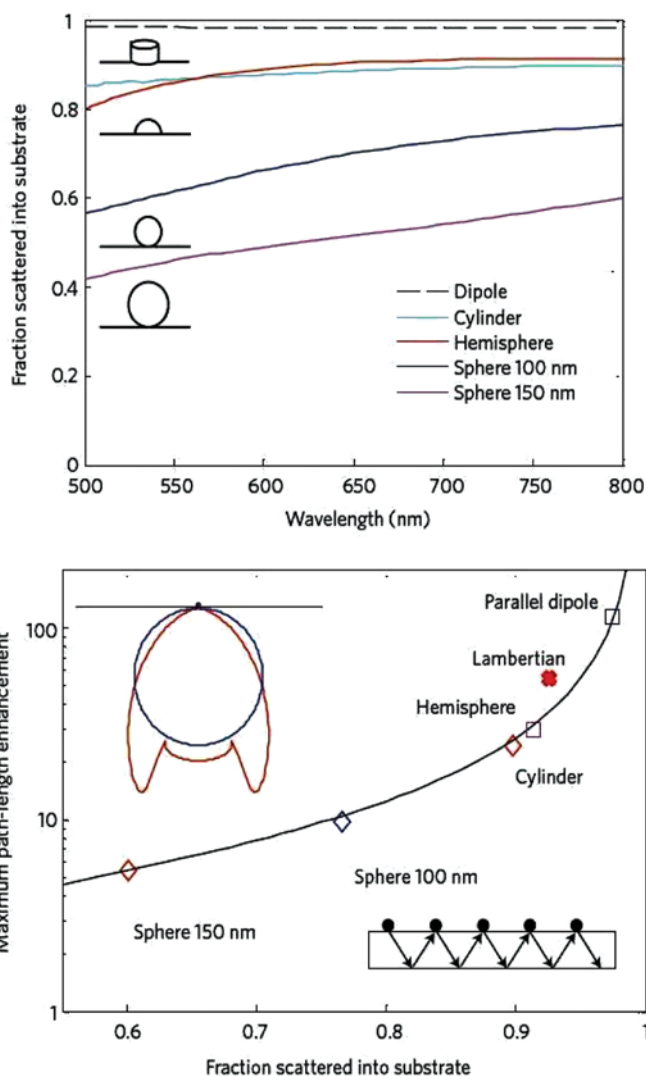


Fig. 11. Sensitivity of plasmon light scattering to nanoparticles’ shape and size. Reprinted by permission from Macmillan Publishers Ltd.: Atwater, H. A., and Polman, A. (2010). Plasmonics for improved photovoltaic devices. *Nature Materials* 9: 205–213. (Figure available in color online.)

formation around the nanoparticle. These plasmons create a strong electric field around the nanoparticle and enhance the absorption in the region contiguous to it. This technique is very useful for OPV because in OPV the diffusion length is short. Thus, the placement of nanoparticles is most beneficial when placed close to the junction (S. Kim et al. 2009). Another factor is that the absorbed light should have a high absorption rate; otherwise, the oscillated plasmons will decay, and the energy will be dispersed (Atwater and Polman 2010). This condition is suitable for OPVs because the materials used have high absorption rate. Figure 12 illustrates the intensity of the near-field close to the nanoparticle surface.

In the third geometry (Figure 10c), the back grated contact can couple the light into a surface plasmon polariton (SPP) mode in which the light will scatter 90° and propagate along the semiconductor adjacent to the metal-semiconductor interface (Atwater and Polman 2010), resulting in an increased chance of light absorption. In the last few years, a good deal of work has been performed to add plasmonic structures to OPVs with the goal of increasing the PCE (Pan and Rothberg 2007). PCEs as high as 5.7% have been demonstrated using this structure (Xue et al. 2004).

Table 1 shows some of the reported efficiencies in various types of organic solar cells. The table demonstrates the development in PCE of OPVs during almost the last four decades. An increase in the PCE of OPVs from 0.001% in 1975 (where the first OPV cell brought to light) to 8.6% in 2012 has been achieved.

11. Carbon Nanotube/Polymer Nanocomposites

While many efforts are currently being pursued in the realm of donor polymer engineering, the acceptor material must also be improved. In the photoactive layer, the conducting

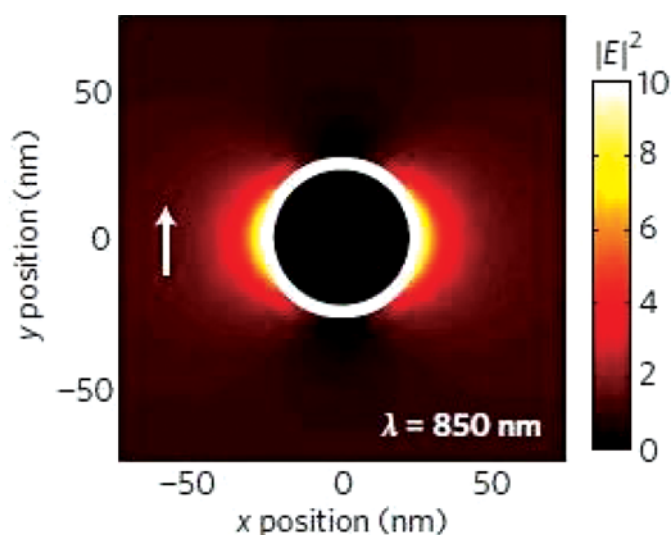


Fig. 12. The enhancement of the near-field close to the nanoparticle surface. Reprinted by permission from Macmillan Publishers Ltd.: Atwater, H. A., and Polman, A. (2010). Plasmonics for improved photovoltaic devices. *Nature Materials* 9: 205–213. (Figure available in color online.)

polymer contributes to the photoconduction process and acts as the exciton generation center, but carbon nanotubes, a carbon allotrope similar to fullerenes, are also reported to contribute to photoconduction (Freitag et al. 2003). Figure 13a shows a TEM image of multi-walled carbon nanotubes (MWCNTs).

The discovery of CNTs by Ijima (1991) generated great interest in exploring the properties of CNTs and their applications. It was found that the incorporation of CNTs into organic conducting polymers could improve the performance of the polymer PV cell (Kymakis and Amaratunga 2002). The research continues to improve the performance (i.e., open circuit voltage, short circuit current, and efficiency) of the CNT-conducting polymer composite PV cell.

CNTs can be applied to two important aspects of OPV devices: as a transparent conductive layer to replace ITO (Lagemaat et al. 2006) and in the active layer as a composite with conducting polymers. When used as a composite material in active layers, CNTs can enhance device efficiency by several orders of magnitude (Kymakis and Amaratunga 2002). When light is shone on an OPV, excitons generated in the conducting polymer diffuse through the polymer to reach the CNT/conducting polymer junction. The latter acts as an exciton dissociation center, and the electrons and holes are transported to the electrodes through CNTs and the conducting polymer, respectively. Even though CNTs improve the characteristics of OPVs, the power conversion efficiency of the CNT/conducting polymer PV cell is still low compared to that of the inorganic PV cell. The reason for this low efficiency is that most of the excitons generated in the conducting polymer recombine before reaching the CNT/conducting polymer junction due to their small diffusion lengths. Reducing the recombination rate of electrons and holes can increase the efficiency of this PV cell, which is accomplished by depositing a very thin (on the order of a few hundred nanometers), uniformly dispersed CNT/conducting polymer photoactive layer. The CNTs used should be highly crystalline and free from metal impurities to prevent the formation of charge traps in the photoactive layer. For optimal performance of a PV cell, the CNTs should be uniformly dispersed in the polymer, and it has been found that the polymer chains wrap around the walls of CNTs creating heterojunction along the wall of CNTs (Motta et al. 2005). This is necessary for efficient charge dissociation at the CNT/polymer junction because of the low exciton diffusion length. Another advantage of well-dispersed CNTs is the formation of percolation paths by CNTs through the composite, which improves the electron transportation and reduces the recombination rate of charges in the active layer. Saini et al. (2009) has shown that the incorporation of MWCNTs in P3HT matrix can drastically improve the structural, morphological, thermal, optical, and electrical properties of P3HT. Moreover, Petre et al. (2010) demonstrated that the presence of MWCNTs in P3HT can influence the dielectric behavior of P3HT polymer, in addition to the increase in crystallization and melting temperatures.

CNTs, especially single-walled carbon nanotubes (SWNTs), show great potential for use in solar cell applications due to

Table 1. Power conversion efficiency of some organic cell

Cell	Type	Architecture	Year	PCE (%)	Reference
Al/chlorophyll- <i>a</i> /Hg	Metal/small molecule/metal	Bilayer	1975	0.001	(Tang and Albrecht 1975)
pentacene/C60	Small molecule/small molecule	Bilayer	2009	1.6	(Pandey and Nunzi 2006)
SubPc/C60	Small molecule/small molecule	Bilayer	2006	2.1	(Mutolo et al. 2006)
M3EH-PPV/CN-ether-PPV	Polymer/polymer	Bilayer	2006	1.3	(Kietzke et al. 2006)
MDMO-PPV:PCBM	Polymer/small molecule	Blend	2001	2.5	(Shaheen et al. 2001)
P3HT:PCBM	Polymer/small molecule	Blend	2005	3	(Y. Kim et al. 2005)
P3HT:PCBM	Polymer/small molecule	Blend	2007	4.3	(Wang et al. 2007)
PBDTTT:PCBM	Polymer/small molecule	Blend	2009	6.77	(Chen et al. 2009)
PBnDT-DTffBT:PCBM	Polymer/small molecule	Ternary blend	2011	7.2	(Zhou et al. 2011)
P3HT:PCBM-PCBTTE ^a	Polymer/small molecule	Ternary blend	2012	4.37	(Lai et al. 2012)
PTB7:PC ₇₁ BM	Polymer/small molecule	Blend	2010	7.4	(Liang et al. 2010)
CuPc/PCBM//P3HT:PTCBI	Tandem	Bilayer//blend	2008	2.79	(C. Zhang et al. 2008)
F4-ZnPc:C ₆₀ ^b //DCV6 T ^c :C ₆₀	Tandem	Blend//blend	2011	4.9	(Meiss et al. 2011)
CuPc/CuPc:C ₆₀ /C ₆₀ //Ag//CuPc/CuPc:C ₆₀ /C ₆₀	Plasmonic tandem	Hybrid ^d //hybrid	2004	5.7	(Xue et al. 2004)
ZnO/P3HT:IC ₆₀ BA ^e /PEDOT:PSS//ZnO/PBDTT-DPP ^f :PC ₇₁ BM/MoO ₃ /Ag	Inverted tandem	Blend//blend	2012	8.62	(Dou et al. 2012)

^aPCBTTE is [6,6]-phenyl-C61-butyricacid2-(2',2'':5'',2'''-terthiophene-5'-yl)ethylester.

^bF4-ZnPc:C60 is fluorinated ZnPc.

^cDCV6 T is α,ω -bis-(dicyanovinyl-sexithiophene)-Bu(1,2,5,6).

^dHybrid in this context is a cell comprised of planner and bulk architectures.

^eIC₆₀BA is indene-C₆₀ bisadduct.

^fPBDTT-DPP is poly{2,6'-4,8-di(5-ethylhexylthienyl)benzo[1,2-b;3,4-b]dithiophene-alt-5-dibutylloctyl-3,6-bis(5-bromothiophen-2-yl)pyrrolo[3,4-c]pyrrole-1,4-dione}.

their unique electrical, optical, mechanical, and structural properties. There are several reasons for using SWNTs in a polymer composite PV cell:

1. The high surface area ($\sim 1600 \text{ m}^2/\text{g}$) of SWNTs (Cinke et al. 2002) provides the opportunity to form numerous heterojunctions between CNTs and the polymer. Since it has been observed that the polymer wraps itself over the CNT surface, exciton dissociation is thought to increase.
2. The SWNTs have diameters of $\sim 1 \text{ nm}$ and lengths in micrometers; therefore, they exhibit a very high aspect ratio ($> 10^3$).
3. Inefficient charge transfer is the main problem with conducting polymer PV cells. The incorporation of SWNTs at low levels establishes percolation pathways, which enhances the carrier mobility.

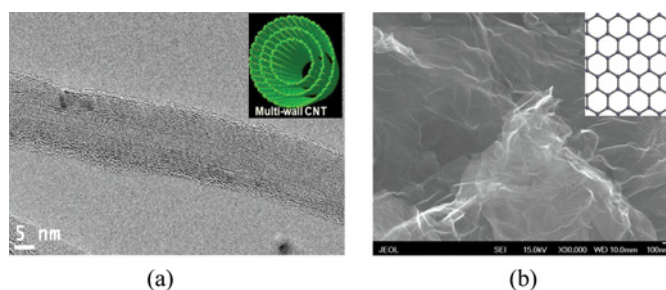


Fig. 13. a) TEM image of a MWCNT of about 20 nm in diameter (inset: schematic representation of a MWCNT); b) SEM image of graphene sheets under x30000 magnification (inset: structural representation of a single graphene sheet). (Figure available in color online.)

4. The diffusion length of excitons in conducting polymers is low; therefore, a percolation network is necessary in a polymer composite, which is provided by electron-acceptor dopants like SWNTs.
5. The electrical conductivity of a SWNT-conducting polymer composite increases by a factor of 10^5 from 0.1 to 0.2% w/w loading (Biercuk et al. 2002).
6. SWNTs provide mechanical strength to the SWNT-conducting polymer composite thin film PV cell. The tensile strength of a SWNT is ~ 20 GPa and the Young's Modulus is ~ 1 GPa (F. Li et al. 2000).
7. SWNTs provide thermal management for the SWNT-conducting polymer composite PV cell. The thermal conductivity of SWNTs (10,10) has been calculated theoretically to be 6600 W/mK (Berber et al. 2000). A 1% w/w SWNT-doped conducting polymer composite showed a 70% increase in thermal conductivity at 40 K over pristine polymer (Cinke et al. 2002).

12. Carbon Nanotube/Polymer Bulk Heterojunction Solar Cells

Kymakis et al. (Kymakis and Amaratunga 2002; Kymakis et al. 2003; Bhattacharyya et al. 2004; Kymakis and Amaratunga 2005) conducted an in-depth study of the CNT/conducting polymer PV cell and explained its operating mechanism. In a pristine polymer PV cell, the construction is composed of ITO/pristine polymer/Al layers. The open circuit voltage in a pristine polymer PV cell is described by the metal-insulator-metal (MIM) model (Tang 1986). In the MIM model, the upper limit of the V_{OC} is the work function difference between the two metal electrodes, that is, ITO ~ 4.7 eV and Al ~ 4.3 eV, which agrees with the measured V_{OC} of 0.35 V. It has been reported that the MIM model is not valid for the CNT/polymer PV cell because this PV cell uses a very thin pristine polymer buffer layer between the ITO and CNT/polymer composite. This thin buffer layer prevents ohmic contact between the ITO and CNT/conducting polymer composite. As a result, because of the ohmic contact between CNT and Al, the maximum V_{OC} of a CNT/polymer PV cell is given by the work function difference of the ITO and CNT layer (Kymakis and Amaratunga 2002). Lately, it was projected that, because the CNTs make an ohmic contact with the metal electrode, the highest V_{OC} that can be achieved is the difference of the HOMO of the conducting polymer and the work function of the CNT with an assumption that all CNTs in the composite are metallic (Bhattacharyya et al. 2004). In addition, it has been stated that the I_{SC} is linearly dependent upon the intensity of incident light whereas the V_{OC} is entirely independent. Because of this, the fill factor has been shown to decrease with an increase in the intensity of the incident light. The V_{OC} measured from two different CNT/polymer PV cell devices will likely not be similar. This is due to several reasons. The first is based on the approach of estimating the V_{OC} where the work function of ITO depends on the manufacturing conditions and environment (Sugiyama et al. 2000). The published values of the ITO work

function vary from 4.1 to 5.5 eV (Park et al. 1996). Another reason which is based on both of the above approaches in estimating the V_{OC} , is that the work function of CNTs is dependent on their diameter, chirality, and type. The work function of SWNTs ranges from 3.4 to 4.0 eV, whereas, for MWNTs, it ranges from 4.6 to 5.1 eV (Gröning et al. 2000).

A variety of V_{OC} , I_{SC} , FF, and PCE values have been reported for OPVs based on CNTs. Kymakis and Amaratunga (2002) constructed an ITO/PEDOT:PSS/P3OT-SWNTs/Al photovoltaic cell with 1% w/w SWNTs (where P3OT is poly(3-octylthiophene)), which shows an I_{SC} of 0.25 mA/cm², V_{OC} of 0.75 V, FF of 0.48 and PCE of 0.1%; on the other hand, a PV cell containing only pristine P3OT shows I_{SC} of 0.7 μ A/cm², V_{OC} of 0.35 V and FF of 0.3. The improved properties are due to several reasons. The conducting polymer-nanotube junctions act as dissociation centers where excitons dissociate into free electrons and holes. In addition, SWNTs provide percolation pathways for the electrons to reach the Al metal electrode. Both P3OT and SWNTs provide electrical transport paths for the charge carriers.

The performance of ITO/P3OT-SWNT/Al and ITO/P3OT-SWNT + NPM (N-(1-pyrenyl)maleimide)/Al photovoltaic cells have also been studied and compared by Kymakis and Amaratunga (2002). Here, the SWNTs were functionalized with NPM, which attaches to the surface of SWNT by π -stacking. The non-contribution of SWNTs to photogeneration is overcome by incorporating this dye at the conducting polymer/nanotube junction. For ITO/P3OT-SWNT + NPM/Al PV cells, the I_{SC} , V_{OC} , FF, and PCE are 0.18 mA/cm², 0.6 V, 0.35 and 0.036%, respectively. Whereas, for ITO/P3OT-SWNT/Al PV cells, the I_{SC} , V_{OC} , FF, and PCE are 5.5 μ A/cm², 0.5 V, 0.28, and 7.5×10^{-4} %. The V_{OC} measured by this structure is greater than that obtained from the pristine conducting polymer PV cell. In the pristine conducting polymer PV cell, the V_{OC} is characterized by the work function difference between the two metal electrodes, that is, ITO (4.7 eV) and Al (4.3 eV), which is 0.4 V. The difference in the V_{OC} of these PV cells lies in their construction. A thin pristine P3OT layer is placed between the ITO and P3OT/SWNT composite active layer that hinders the short circuit between the metal electrodes provided by SWNT percolation pathways. In P3OT/SWNT composite PV cells, the maximum V_{OC} is the difference between the work function of SWNT (4.6 eV) (Zhao et al. 2002) and the HOMO energy level of P3OT (5.25 eV) (Yoshino et al. 1998): 0.65 eV. Because the work function of SWNTs varies with chirality, type (metal or semiconductor), and diameter (Okazaki et al. 2003), the V_{OC} is likely to vary from device to device.

Landi et al. (2005) constructed an ITO/P3OT/SWNT-P3OT/Al PV cell, and the I-V characteristics were studied under simulated AM0 illumination. The I_{SC} was shown to increase one order of magnitude for 0.1% w/w SWNT-P3OT device when compared with pristine polymer device. A further 50% improvement was observed when the doping concentration of SWNTs was increased from 0.1% w/w to 1.0% w/w in the polymer composite; an open

circuit voltage, V_{OC} , of 0.98 V and a short circuit current, I_{SC} , of 0.12 mA/cm² for a 1.0% w/w SWNT-P3OT composite was measured. By incorporating SWNTs, the electrical conductivity also increased (Landi et al. 2002), which improved the carrier transport and eventually the I_{SC} . In addition, the high V_{OC} was attributed to the purity and defect density of SWNTs. It has also been proposed that the SWNT-P3OT PV cell performance can be improved by the attachment of semiconductor nanoparticle (e.g., CdSe) quantum dots (QDs) to SWNTs (Haremza et al. 2002), which enhances the charge separation and carrier transport. The semiconducting QDs provide an intermediate band to match the energy bands between the conducting polymer and CNTs. The biggest hurdle in this approach is the wide range of band gaps and electron affinities available for most of the polymers, QDs, and CNTs. The wide range of band gap is due to the size-dependent, electro-optical properties of nanoscale materials, variations in the CNTs' chirality and purity, variations in the defect densities of both CNTs and QDs, and variations in polymers that arise based on their processing conditions (Raffaella et al. 2005).

A study of nanotube/conducting polymer composite PV cells reported a high V_{OC} (1.81 V) and greatly improved efficiency (1.41%) (Patyk et al. 2007). The reason for this enhancement in V_{OC} and efficiency is the modification in the construction of the SWNT/conducting polymer composite PV cell: expensive ITO is replaced by cheaper fluorine-doped tin-oxide (FTO); a polybithiophene (PBT) layer is introduced between the CNT/conducting polymer composite active layer and transparent electrode (FTO); the SWNTs are modified with 2-(2-tienyl)ethanol to form SWNT-TIOPH; and a Ca/Al electrode is used.

Apart from the research described above, researchers and scientists are exploring a variety of new ways to harvest the solar spectrum using CNT/conducting polymer PV cells. The material selection ranges from poly(alkylthiophenes) (including P3HT, P3OT, etc.), PEDOT:PSS to MEH-PPV. In addition, only SWNTs have been used in these PV cells, there is still room for research with double-walled carbon nanotubes (DWNTs) and multi-walled carbon nanotubes (MWNTs).

The V_{OC} model for the CNT/polymer PV cell is different from the organic polymer PV cell. In the CNT/polymer PV cell, the V_{OC} is the work function difference of the CNT and the HOMO level of the polymer. In addition, the best efficiency is achieved by using 1% w/w SWNTs in the polymer composite. This efficiency can be enhanced by attachment of QDs to the walls of CNTs. A review of the literature shows that there is a plethora of undiscovered potential in the CNT/conducting polymer PV cell.

13. Graphene/Polymer Bulk Heterojunction Solar Cells

Graphene is a sheet of honeycombed carbon atoms of single atom thickness. A schematic image of a graphene sheet is shown in Figure 13b. Graphene possesses remarkable photonic properties, such as high transparency and a wide absorp-

tion spectral range, as well as outstanding electronic and mechanical properties (Neto et al. 2009). As a result, extensive interest has developed in applying graphene to optoelectronic devices. The two-dimensionality and structural flatness make graphene sheets ideal candidates for thin-film devices. Despite their high aspect ratio, the cylindrical nature of CNTs prevents the formation of an ultra-wide interfacial area; thus, a nanocomposite of P3OT/graphene has been suggested by Liu et al. (2008) as an alternative. This has been the motivation for several publications about P3OT/graphene and P3HT/graphene nanocomposites (Liu et al. 2008; Q. Liu et al. 2009; Chang et al. 2010; Yang et al. 2010; Yu et al. 2010; Potts et al. 2011; Saini et al. 2012). Since the incorporation of graphene in conducting polymers results in a nanocomposite with a large interfacial surface area, the amount of graphene can be reduced by comparison with the nanotube concentration required for the CNT/polymer composites. Moreover, graphene has higher mobility and conductivity than CNTs and may function better as an electron acceptor. It has also been reported that graphene is more easily dispersed within the P3HT matrix compared to CNTs (Chang et al. 2010). Preliminary studies of graphene/polymer cells have produced encouraging results and higher PCE than those recorded for CNTs/polymer cells. Liu et al. (2008) have reported a 1.4% PCE for the architecture ITO/PEDOT:PSS/P3OT:graphene/LiF/Al.

14. Carbon Nanotubes as Active Material in Hybrid Solar Cells

Carbon allotropes possessing diverse properties allow carbonaceous materials to be touted for use in a variety of applications. Carbon is found in various elemental forms, such as diamond, graphite, graphene, fullerenes, and CNTs. All of these forms of carbon exhibit a rich variety of electronic and physical properties: Diamond is insulating (Robertson 2002), graphite and graphene are either metallic or semi-metallic (Novoselov et al. 2004; Geim and Novoselov 2007), fullerenes (e.g., C₆₀) are semiconducting (Kroto et al. 1985; Hirsch and Brettreich 2005), and CNTs show metallic and semiconducting behavior depending upon chirality (Saito et al. 1998; Baughman et al. 2002; Lai et al. 2012) and the tube diameter/number. Empirically, the CNT bandgap is related to its diameter according to the following (Jia et al. 2008):

$$E_g = \frac{7.98}{d} \quad (4)$$

where d is the tube diameter in angstroms. In addition to their unique electronic properties, these different carbon forms also show some interesting optical, physical, and chemical properties.

Since the discovery and research development in organic solar cells, C₆₀ and its derivatives have become one of the most widely used electron acceptor material in polymer/fullerene composites. A p-n junction is the basis of most solar cells for photocurrent generation (except for non p-n junction excitonic donor-acceptor organic solar cells). The acid-purified CNTs have been shown to have p-type

behavior (Dürkop et al. 2004). The MWNTs/n-Si heterojunction has been demonstrated to have a rectifying current-voltage behavior (Hu et al. 1999), and, recently, double-walled carbon nanotubes (DWNTs) have also demonstrated a photovoltaic effect by forming numerous heterojunctions with n-type silicon (Wei et al. 2007). SWCNTs and boron-doped SWCNTs have been used as active layers on silicon to fabricate low-cost p-SWCNTs/n-Si heterojunction solar cells (Li et al. 2009; Li et al. 2008; Saini et al. 2011). Bourdo et al. (2010) has proven that polyaniline (PANI) doped with tanninsulfonic acid can function as a heterojunction materials for PANI/n-Si solar cells. SWCNTs can also be used as a charge collector mat on top of PANI/n-Si heterojunction solar cells. The presence of SWCNTs is reported to double the power conversion efficiency (Bourdo et al. 2012). Recent attempts have been made to produce n-type SWCNTs by polymer functionalization, which has led to the fabrication of n-SWCNTs/p-Si heterojunctions (Li et al. 2010). CNTs are also of great interest in solar cell applications because of their unique properties: high aspect ratio, semiconducting or metallic, high carrier density and mobilities, reduced carrier transport scattering, the presence of wide range of direct bandgaps matching the solar spectrum and strong photo absorption ranging from infrared to ultraviolet region, which are essential for photovoltaics. Furthermore, a single carbon nanotube can have multiple bandgaps which increases the light absorption.

15. Conclusions

After more than 25 years of research and development, organic solar cells are now a substantially improved technology. These improvements have resulted in an increase in the PCE of OPVs from 0.001% in 1975 (when the first OPV cell was described) to 8.6% in 2012. As PCE increases, OPV research and technology will attract an army of researchers, resulting in cost reduction and could lead to replacement of inorganic PVs by OPVs in many cases. Since markets demand that an efficiency of 10% or higher is necessary for commercial viability, the research efforts into OPVs continues in earnest.

The three major advantages of using organic materials are: a) the expected high-efficiency per unit cost ratio, b) the simplicity in fabrication and processing, and c) the mechanical flexibility of these materials. These advantages spur intensive research to overcome the shortcomings of OPVs. The limitations with respect to OPV efficiency stem from the short diffusion length and from low absorption of the active layer. Using a tandem architecture incorporated with plasmons can extend the absorption range to the entire solar spectrum and enhance the absorption while keeping active layer thickness relatively thin. CNTs and graphene have been studied for replacement of fullerenes (electron acceptors) and/or transparent electrodes and organic cells made from CNTs/polymer nanocomposites are expected to be at the forefront of the next generation of solar cell materials. These are just some examples of promising configurations

that will enable organic solar cells to be economically competitive with conventional inorganic solar cells and perhaps replace them in the future.

Acknowledgment

The financial support from the Arkansas Science & Technology Authority (Grant # 08-CAT-03), and the Department of Energy (DE-FG36-06GO86072) and National Science Foundation (NSF/EPS-1003970) is greatly appreciated. The editorial assistance of Marinelle Ringer is also acknowledged.

References

- Abdulrazzaq, O., S. Bourdo, V. Saini, V. Bairy, E. Dervishi, T. Viswanathan, and A. S. Biris. 2013. Optimization of protonation level of polyaniline-based hole transport layer in bulk-heterojunction organic solar cells. *Energy Technology*. Accepted for publication, DOI 10.1002/ente.201300058
- Alam, M., and S. Jenekhe. 2004. Efficient solar cells from layered nanostructures of donor and acceptor conjugated polymers. *Chemistry of Materials* 16(23):4647–4656.
- Arias, A., J. MacKenzie, R. Stevenson, M. Halls, M. Inbasekaran, E. Woo, D. Richards, and R. Friend. 2001. Photovoltaic performance and morphology of polyfluorene blends: A Combined microscopic and photovoltaic investigation. *Macromolecules* 34(17):6005–6013.
- Atwater, H., and A. Polman. 2010. Plasmonics for improved photovoltaic devices. *Nature Materials* 9:205–213.
- Aziz, E., A. Vollmer, S. Eisebitt, W. Eberhardt, P. Pingel, D. Neher, and N. Koch. 2007. Localized charge transfer in a molecularly doped conducting polymer. *Advanced Materials* 19:3257–3260.
- Bagui, A., and S. Iyer. 2011. Effect of solvent annealing in the presence of electric field on P3HT:PCBM films used in organic solar cells. *IEEE Transactions on Electron Devices* 58(11):4061–4066.
- Barth, S., and H. Bassler. 1997. Intrinsic photoconduction in PPV type conjugated polymers. *Physics Review Letters* 79(22):4445–4448.
- Baughman, R., A. Zakhidov, and W. Heer. 2002. Carbon nanotubes—The route toward applications. *Science* 297(5582):787–792.
- Berber, S., Y. Krown, and D. Tomanek. 2000. Unusually high thermal conductivity of carbon nanotubes. *Physics Review Letters* 84(20):4613–4616.
- Bhattacharyya, S., E. Kymakis, and G. Amaratunga. 2004. Photovoltaic properties of dye functionalized single-wall carbon nanotube/conjugated polymer devices. *Chemistry of Materials* 16(23):4819–4823.
- Biercuk, M., M. Llaguno, M. Radosavljevic, J. Hyun, A. Johnson, and J. Fischer. 2002. Carbon nanotube composites for thermal management. *Applied Physics Letters* 80(15):2767–2769.
- Bourdo, S., V. Saini, J. Piron, I. Al-Brahim, C. Boyer, J. Rioux, V. Bairy, A. S. Biris, and T. Viswanathan. 2012. Photovoltaic device performance of single-walled carbon nanotube and polyaniline films on n-Si: Device structure analysis. *ACS Appl. Mater. Interfaces* 4: 363–368.
- Bourdo, S., V. Saini, B. Warford, F. Prou, V. Bairy, Z. Li, A. S. Biris, and T. Viswanathan. 2010. Tanninsulfonic acid doped polyaniline as a novel heterojunction material in hybrid organic/inorganic solar cells. Materials Research Society Symposium Proceedings Vol. 1270, Organic Photovoltaics and Related Electronics, Paper No. 1270-HH14–54.
- Brabec, C., and J. Durrant. 2008. Solution-processed organic solar cells. *MRS Bulletin* 33:670–675.
- Brabec, C., S. Gowrisanker, J. Halls, D. Laird, S. Jia, and S. Williams. 2010. Polymer-fullerene bulk-heterojunction solar cells. *Advanced Materials* 22(34):3839–3856.
- Camaioni, N., G. Ridolfi, V. Fattori, L. Favaretto, and G. Barbarella. 2005. Branched thiophene-based oligomers as electron acceptors

- for organic photovoltaics. *Journal of Materials Chemistry* 15(22):2220–2225.
- Catchpole, K., and A. Polman. 2008. Design principles for particle plasmon enhanced solar cells. *Applied Physics Letters* 93:191113–191115.
- Chang, Y., S. Yu, C. Liu, and R. Tsiang. 2010. Morphological and optoelectronic characteristics of nanocomposites comprising graphene nanosheets and poly(3-hexylthiophene). *Journal of Nanoscience and Nanotechnology* 10(10):6520–6526.
- Chapin, D., C. Fuller, and G. Pearson. 1954. A new silicon p-n junction photocell for converting solar radiation into electrical power. *Journal of Applied Physics* 25:676–677.
- Chen, H., J. Hou, S. Zhang, Y. Liang, G. Yang, Y. Yang, L. Yu, Y. Wu, and G. Li. 2009. Polymer solar cells with enhanced open-circuit voltage and efficiency. *Nature Photonics* 3:649–653.
- Cinke, M., J. Li, B. Chen, A. Cassel, L. Delzeit, J. Han, and M. Meyyappan. 2002. Pore Structure of raw and purified HiPco single-walled carbon nanotubes. *Chemical Physics Letters* 365:69–74.
- Dennler, G., H. Prall, R. Koeppel, M. Egginger, R. Autengruber, and N. Sariciftci. 2006. Enhanced spectral coverage in tandem organic solar cells. *Applied Physics Letters* 89(7):073502–073504.
- Dou, L., J. You, J. Yang, C. Chen, Y. He, S. Murase, T. Moriarty, K. Emery, G. Li, and Y. Yang. 2012. Tandem polymer solar cells featuring a spectrally matched low-bandgap polymer. *Nature Photonics* 6:180–185.
- Drechsel, J., B. Mannig, F. Kozlowski, M. Pfeiffer, K. Leo, and H. Hoppe. 2005. Efficient organic solar cells based on a double p-i-n architecture using doped wide-gap transport layers. *Applied Physics Letters* 86(24):244102–244104.
- Dürkop, T., S. Getty, E. Cobas, and M. Fuhrer. 2004. Extraordinary mobility in semiconducting carbon nanotubes. *Nano Letters* 4:35–39.
- Edwards, E. 2007. Organic solar cells: A review. EE293a Program, Stanford University.
- Ferry, V., M. Verschuuren, H. Li, E. Verhagen, R. Walters, R. Schropp, H. Atwater, and A. Polman. 2010. Light trapping in ultrathin plasmonic solar cells. *Optics Express* 18(102):A237–A245.
- Fonash, S. 1981. *Solar Cell Device Physics*. New York: Wiley.
- Freitag, M., Y. Martin, J. Misewich, R. Martel, and P. Avouris. 2003. Photoconductivity of single carbon nanotubes. *Nano Letters* 3(8):1067–1071.
- Galagan Y., Date J. D. Moet, Dorothee C. Hermes, Paul W. M. Blom, and Ronn Andriessen. 2012. Large area ITO-free organic solar cells on steel substrate. *Organic Electronics* 13:3310–3314.
- Geim, A., and K. Novoselov. 2007. The rise of graphene. *Nature Materials* 6:183–191.
- Goetzberger, A. 1981. Optical confinement in thin Si-solar cells by diffuse back reflectors. 15th IEEE Photovoltaic Specialists Conference (Institute of Electrical and Electronics Engineers, New York), pp. 867–870.
- Gröning, O., O. Kuttel, C. Emmenegger, P. Gröning, and L. Schlapbach. 2000. Field emission properties of carbon nanotubes. *Journal of Vacuum Science & Technology B* 18:665–678.
- Halls, J., and R. Friend. 1997. The photovoltaic effect in a poly (P-phenylenevinylene)/perylene heterojunction. *Synthetic Metals* 85:1307–1308.
- Halls, J., K. Pichler, R. Friend, S. Moratti, and A. Holmes. 1996. Exciton diffusion and dissociation in a poly(P-phenylenevinylene)/C60 heterojunction photovoltaic cell. *Applied Physics Letters* 68(22):3120–3122.
- Halls, J., C. Walsh, N. Greenham, E. Marseglia, R. Friend, S. Moratti, and A. Holmes. 1995. Efficient photodiodes from interpenetrating polymer networks. *Nature* 376:498–500.
- Haremza, J., M. Hahn, T. Krauss, S. Chen, and J. Calcines. 2002. Attachment of single CdSe nanocrystals to individual single-walled carbon nanotubes. *Nano Letters* 2:1253–1258.
- Hashimoto, Y., and M. Hamagaki. 2006. Effect of oxygen plasma treatment of indium tin oxide for organic solar cell. *Electrical Engineering in Japan* 154(4):379–384.
- Hau, S., H. Yip, and A. Jen. 2010. A review on the development of the inverted polymer solar cell architecture. *Polymer Reviews* 50:474–510.
- Heeger, A. 2001. Nobel lecture: Semiconducting and metallic polymers: The fourth generation of polymeric materials. *Reviews of Modern Physics* 73(3):681–700.
- Hirsch, A., and M. Brettreich. 2005. *Fullerenes: Chemistry and Reactions*. Wiley-VCH Verlag GmbH & Co. KGaA.
- Hoppe, H., and N. Sariciftci. 2004. Organic solar cells: An overview. *Journal of Materials Research* 19(7):1924–1945.
- Hu, J., M. Ouyang, P. Yang, and C. Lieber. 1999. Controlled growth and electrical properties of heterojunctions of carbon nanotubes and silicon nanowires. *Nature* 399:48–51.
- Iijima, S. 1991. Helical microtubules of graphitic carbon. *Nature* 354:56–58.
- Jia, Y., J. Wei, K. Wang, A. Cao, Q. Shu, X. Gui, Y. Zhu, D. Zhuang, G. Zhang, B. Ma, L. Wang, W. Liu, Z. Wang, J. Luo, and D. Wu. 2008. Nanotube-silicon heterojunction solar cells. *Advanced Materials* 20:4594–4598.
- Jing, X., D. Zhenbo, L. Chunjun, X. Denghui, X. Ying, and G. Dong. 2005. Effect of LiF buffer layer on the performance of organic electroluminescent devices. *Physica E* 28:323–327.
- Jorgensen, M., K. Norrman, and F. Krebs. 2008. Stability/degradation of polymer solar cells. *Solar Energy Materials & Solar Cells* 92:686–714.
- Kalowekamo, J., and E. Baker. 2009. Estimating the manufacturing cost of purely organic solar cells. *Solar Energy* 83(8):1224–1231.
- Kerp, H., H. Donker, R. Koehorst, T. Schaafsma, and E. Faasse. 1998. Exciton transport in organic dye layers for photovoltaic applications. *Chemical Physics Letters* 298:302–308.
- Kietzke, T. 2007. Recent advances in organic solar cells. *Advances in OptoElectronics* 1–15.
- Kietzke, T., D. Egbe, H. Rhold, and D. Neher. 2006. Comparative study of M3EH-PPV-based bilayer photovoltaic devices. *Macromolecules* 39(12):4018–4022.
- Kietzke, T., H. Horhold, and D. Neher. 2005. Efficient polymer solar cells based on M3EH-PPV. *Chemistry of Materials* 17(26):6532–6537.
- Kim, Y., S. Choulis, J. Nelson, D. Bradley, S. Cook, and J. Durrant. 2005. Device annealing effect in organic solar cells with blends of regioregular poly(3-hexylthiophene) and soluble fullerene. *Applied Physics Letters* 86(6):063502–063504.
- Kim, J., K. Lee, N. Coates, D. Moses, T. Nguyen, M. Dante, and A. Heeger. 2007. Efficient tandem polymer solar cells fabricated by all-solution processing. *Science* 317(5835):222–225.
- Kim, S., S. Na, J. Jo, D. Kim, and Y. Nah. 2009. Plasmon enhanced performance of organic solar cells using electrodeposited Ag nanoparticles. *Applied Physics Letters* 93(7):073307–073309.
- Kroto, H., J. Heath, S. O'Brien, R. Curl, and R. Smalley. 1985. C60: Buckminsterfullerene. *Nature* 318:162–163.
- Kymakis, E., I. Alexandrou, and G. Amaratunga. 2003. High open-circuit voltage photovoltaic devices from carbon-nanotube-polymer composites. *Journal of Applied Physics* 93:1764–1768.
- Kymakis, E., and G. Amaratunga. 2002. Single-wall carbon nanotube/conjugated polymer photovoltaic devices. *Applied Physics Letters* 80(1):112–114.
- Kymakis, E., and G. Amaratunga. 2005. Carbon nanotubes as electron acceptors in polymeric photovoltaics. *Rev. Advanced Materials Science* 10:300–305.
- Lagemaat, J., T. Barnes, G. Rumbles, S. Shaheen, T. Coutts, C. Weeks, I. Levitsky, J. Peltola, and P. Glatkowski. 2006. Organic solar cells with carbon nanotubes replacing In2O3:Sn as the transparent electrode. *Applied Physics Letters* 88(23):233503–233505.
- Lai, Y., T. Higashihara, J. Hsu, M. Ueda, and W. Chen. 2012. Enhancement of power conversion efficiency and long-term stability of P3HT/PCBM solar cells using C60 derivatives with thiophene units as surfactants. *Solar Energy Materials & Solar Cells* 97:164–170.
- Landi, B., R. Raffaele, L. Castro, and S. Bailey. 2005. Single-wall carbon nanotube-polymer solar cells. *Progress in Photovoltaics* 13:165–172.

- Landi, B., R. Raffaele, M. Heben, J. Alleman, W. VanDeveer, and T. Gennett. 2002. Single wall carbon nanotube-nafion composite actuators. *Nano Letters* 2(11):1329–1332.
- Li, F., H. Cheng, S. Bai, G. Su, and M. Dresselhaus. 2000. Tensile strength of single-walled carbon nanotubes directly measured from their macroscopic ropes. *Applied Physics Letters* 77(20):3161–3163.
- Li, J., F. Dierschke, J. Wu, A. Grimsdale, and K. Mullen. 2006. Poly (2,7-Carbazole) and Perylene tetracarboxydiimide: A promising donor/acceptor pair for polymer solar cells. *Journal of Materials Chemistry* 16(1):96–100.
- Li, Z., V. Kunets, V. Saini, Y. Xu, E. Dervishi, G. Salamo, A. R. Biris, and A. S. Biris. 2008. SOCl_2 enhanced photovoltaic conversion of single wall carbon nanotube/n-silicon heterojunctions. *Applied Physics Letters* 93(24):243117–243117-3.
- Li, Z., V. Kunets, V. Saini, Y. Xu, E. Dervishi, G. Salamo, A. R. Biris, and A. S. Biris. 2009. Light-harvesting using high density p-Type single wall carbon nanotube/n-type silicon heterojunctions. *ACS Nano* 3(6):1407–1414.
- Li, Z., V. Saini, E. Dervishi, V. Kunets, J. Zhang, Y. Xu, A. R. Biris, G. Salamo, and A. S. Biris. 2010. Polymer functionalized n-type single wall carbon nanotube photovoltaic devices. *Applied Physics Letters* 96:033110–033112.
- Liang, Y., Z. Xu, J. Xia, S. Tsai, Y. Wu, G. Li, C. Ray, and L. Yu. 2010. For the bright future-bulk heterojunction polymer solar cells with power conversion efficiency of 7.4%. *Advanced Materials* 22:E135–E138.
- Liu, Q., Z. Liu, X. Zhang, L. Yang, N. Zhang, G. Pan, S. Yin, Y. Chen, and J. Wei. 2009. Polymer photovoltaic cells based on solution-processable graphene and P3HT. *Advanced Functional Materials* 19:894–904.
- Liu, Q., Z. Liu, X. Zhang, N. Zhang, L. Yang, S. Yin, and Y. Chen. 2008. Organic photovoltaic cells based on an acceptor of soluble graphene. *Applied Physics Letters* 92:223303–223305.
- Liu, Z., Q. Liu, Y. Huang, Y. Ma, S. Yin, X. Zhang, W. Sun, and Y. Chen. 2008. Organic photovoltaic devices based on a novel acceptor material: Graphene. *Advanced Materials* 20:3924–3930.
- Ma, W., C. Yang, X. Gong, K. Lee, and A. Heeger. 2005. Thermally stable, efficient polymer solar cells with nanoscale control of the interpenetrating network morphology. *Advanced Functional Materials* 15(10):1617–1622.
- Meiss, J., T. Menke, K. Leo, C. Uhrich, W. Gnehr, S. Sonntag, M. Pfeiffer, and M. Riede. 2011. Highly efficient semitransparent tandem organic solar cells with complementary absorber materials. *Applied Physics Letters* 99:043301–043303.
- Motta, N., E. Waclawik, R. Goh, and J. Bell. 2005. Nanotube-polymer solar cells—An alternative to silicon. *Bollettino della Comunità Scientifica in Australasia* 16:15–20.
- Mühlbacher, D., M. Scharber, M. Morana, Z. Zhu, D. Waller, R. Gaudiana, and C. Brabec. 2006. High photovoltaic performance of a low-bandgap polymer. *Advanced Materials* 18(21):2884–2889.
- Mutolo, K., E. Mayo, B. Rand, S. Forrest, and M. Thompson. 2006. Enhanced open-circuit voltage in subphthalocyanine/C60 organic photovoltaic cells. *Journal of the American Chemistry Association* 128(25):8108–8109.
- Nara, S., and Y. Sakaguchi. 2003. Newly developed multicrystalline silicon wafer with diffusion length over 250 μm . photovoltaic energy conversion, 1483–1485. Proceedings of 3rd World Conference, May 18.
- Neto, A., F. Guinea, N. Peres, K. Novoselov, and A. Geim. 2009. The electronic properties of graphene. *Reviews of Modern Physics* 81:109–162.
- Nielsen, O. 1980. Current mechanism of tunnel M.I.S, solar cells. *IEE Proceedings* 127(6):301–307.
- Novoselov, K., A. Geim, S. Morozov, D. Jiang, Y. Zhang, S. Dubonos, I. Grigorieva, and A. Firsov. 2004. Electric field effect in atomically thin carbon films. *Science* 306(5696):666–669.
- Okazaki, K., Y. Nakato, and K. Murakoshi. 2003. Absolute potential of the Fermi level of isolated single-walled carbon nanotubes. *Physics Reviews B* 68:035434–035438.
- Pan, S., and L. Rothberg. 2007. Plasmon enhancement of organic photovoltaic efficiency in tandem cells of pentacene/C60. *Proceedings of SPIE* 6641:664109-1–664109-7.
- Pandey, A., and J. Nunzi. 2006. Efficient flexible and thermally stable pentacene/C60 small molecule based organic solar cells. *Applied Physics Letters* 89(21):213506–213508.
- Park, Y., V. Choong, Y. Gao, B. Hsieh, and C. Tang. 1996. Work function of indium tin oxide transparent conductor measured by photoelectron spectroscopy. *Applied Physics Letters* 68:2699–2701.
- Patyk, R., B. Lomba, A. Nogueira, C. Furtado, A. Santos, R. Mello, L. Micaroni, and I. Hummelgen. 2007. Carbon nanotube-polybithiophene photovoltaic devices with high open-circuit voltage. *Physica status solidi (Rapid Research Letters)* 1(1):R43–R45.
- Peet, J., J. Kim, N. Coates, W. Ma, D. Moses, A. Heeger, and G. Bazan. 2007. Efficiency enhancement in low-bandgap polymer solar cells by processing with alkane dithiols. *Nature Materials* 6:497–500.
- Petre, A., S. Diahm, E. Reyes-Melo, V. Saini, Z. Li, E. Dervishi, Y. Xu, and A. S. Biris. 2010. Dielectric behavior of poly(3-hexylthiophene)/carbon nanotube composites by broadband dielectric spectroscopy. *IEEE Transactions on Industry Applications* 46: 627–633.
- Peumans, P., S. Uchida, and S. Forrest. 2003. Efficient bulk heterojunction photovoltaic cells using small-molecular-weight organic thin films. *Nature* 425:158–162.
- Peumans, P., A. Yakimov, and S. Forrest. 2003. Small molecular weight organic thin-film photodetectors and solar cells. *Journal of Applied Physics* 93:3693–3723.
- Potts, J., D. Dreyer, C. Bielawski, and R. Ruoff. 2011. Graphene-based polymer nanocomposites. *Polymer* 52(1):5–25.
- Raffaele, R., B. Landi, C. Evans, S. Castro, and S. Bailey. 2005. Quantum dot-single wall carbon nanotube complexes for polymeric solar cells. Photovoltaic Specialists Conference, 74–77. Conference Record of the 31st IEEE, January 3–7.
- Robertson, J. 2002. Diamond-like amorphous carbon. *Materials Science and Engineering* 37(4–6):129–281.
- Rowell, M., M. Topinka, M. McGehee, H. Prall, G. Denler, N. Sariciftci, L. Hu, and G. Gruner. 2006. Organic solar cells with carbon nanotube network electrodes. *Applied Physics Letters* 88:233506-1–233506-3.
- Saini, V., O. Abdulrazzaq, S. Bourdo, E. Dervishi, A. Petre, V. Bairi, L. Schnackenberg, T. Viswanathan, and A. S. Biris. 2012. Structural and optoelectronic properties of P3HT-graphene composites prepared by in-situ oxidative polymerization. *Journal of Applied Physics* 112:054327.
- Saini, V., Z. Li, S. Bourdo, E. Dervishi, Y. Xu, X. Ma, V. Kunets, G. Salamo, T. Viswanathan, A. R. Biris, D. Saini, and A. S. Biris. 2009. Electrical, optical and morphological properties of P3HT-MWNT nanocomposite prepared by in-situ polymerization. *Journal of Physical Chemistry C* 113(19):8023–8029.
- Saini, V., Z. Li, S. Bourdo, V. Kunets, S. Trigwell, A. Couraud, J. Rioux, C. Boyer, V. Nteziyaremye, E. Dervishi, A. R. Biris, G. Salamo, T. Viswanathan, and A. S. Biris. 2011. Photovoltaic devices based on high density boron-doped single-walled carbon nanotube/n-Si heterojunctions. *Journal of Applied Physics* 109:014321.
- Saito, R., G. Dresselhaus, and M. Dresselhaus. 1998. *Physical properties of carbon nanotubes*. London: Imperial College Press.
- Scharber, M., D. Mühlbacher, M. Koppe, P. Denk, C. Waldauf, A. Heeger, and C. Brabec. 2006. Design rules for donors in bulk-heterojunction solar cells-towards 10% energy-conversion efficiency. *Advanced Materials* 18:789–794.
- Schulze, K., C. Uhrich, R. Schuppel, K. Leo, M. Pfeiffer, E. Brier, E. Reinold, and P. Bäuerle. 2006. Efficient vacuum deposited organic solar cells based on a new low-bandgap oligothiophene and fullerene C60. *Advanced Materials* 18:2872–2875.

- Shaheen, S., C. Brabec, N. Sariciftci, F. Padinger, T. Fromherz, and J. Hummelen. 2001. 2.5% efficient organic plastic solar cells. *Applied Physics Letters* 78:841–843.
- Shin, R., T. Kietzke, S. Sudhakar, A. Dodabalapur, Z. Chen, and A. Sellinger. 2007. N-type conjugated materials based on 2-vinyl-4,5-dicyanoimidazoles and their use in Solar cells. *Chemistry of Materials* 19(8):1892–1894.
- Shin, W., H Jeong, M. Kim, S. Jin, M. Kim, J. Lee, J. Lee, and Y. Gal. 2006. Effects of functional groups at perylene diimide derivatives on organic photovoltaic device application. *J. Mater. Chem.* 16(4):384–390.
- Shrotriya, V., E. Wu, G. Li, Y. Yao, and Y. Yang. 2006. Efficient light harvesting in multiple-device stacked structure for polymer solar cells. *Applied Physics Letters* 88:064104-1–064104-3.
- Solarmer Energy Inc. 2009. <http://www.solarmer.com/index.php> (accessed on May 7, 2012).
- Spire pushes solar cell record to 42.3%. 2010. <http://optics.org/news/1/5/5.7.10.2010>. (accessed on May 7, 2012).
- Sugiyama, K., H. Ishii, Y. Ouchi, and K. Seki. 2000. Dependence of indium-tin-oxide work function on surface cleaning method as studied by ultraviolet and x-ray photoemission spectroscopies. *Journal of Applied Physics* 87:295–298.
- Sun, Y., G. Welch, W. Leong, C. Takacs, G. Bazan, and A. Heeger. 2012. Solution-processed small-molecule solar cells with 6.7% efficiency. *Nature Materials* 11:44–48.
- Tang, C. 1986. Two-Layer Organic Photovoltaic Cell. *Applied Physics Letters* 48(2):183–185.
- Tang, C., and A. Albrecht. 1975. Photovoltaic effects of metal-chlorophyll-a-metal sandwich cells. *J. Chem. Phys.* 62:2139–2149.
- Tao, M. 2008. Inorganic photovoltaic solar cells: Silicon and beyond. *The Electrochemical Society Interface* 30–35.
- Vandewal, K., K. Tvingstedt, A. Gadisa, O. Inganäs, and J. Manca. 2009. On the origin of the open-circuit voltage of polymer–fullerene solar cells. *Nature Materials* 8:904–909.
- Wang, W., H. Wu, C. Yang, C. Luo, Y. Zhang, J. Chen, and Y. Cao. 2007. High-efficiency polymer photovoltaic devices from regioregular-poly(3-hexylthiophene-2,5-diyl) and [6,6]-phenyl-C61-butyric acid methyl ester processed with oleic acid surfactant. *Applied Physics Letters* 90(18):183512–183514.
- Wei, J., Y. Jia, Q. Shu, Z. Gu, K. Wang, D. Zhuang, G. Zhang, Z. Wang, J. Luo, A. Cao, and D. Wu. 2007. Double-Walled Carbon Nanotube Solar Cells. *Nano Letters* 7(8):2317–2321.
- World Community Grid. 2010. <http://www.worldcommunitygrid.org/help/viewSearch.do?searchString=electrons> (accessed May 7, 2012).
- Xia, Y., L. Wang, X. Deng, D. Li, X. Zhu, and Y. Cao. 2006. Photocurrent response wavelength up to 1.1 μm from photovoltaic cells based on narrow-band-gap conjugated polymer and fullerene derivative. *Applied Physics Letters* 89:081106–081108.
- Xue, J., B. Rand, S. Uchida, and S. Forrest. 2004. Asymmetric tandem organic photovoltaic cells with hybrid planar-mixed molecular heterojunctions. *Applied Physics Letters* 85:5757–5759.
- Yang, Z., X. Shi, J. Yuan, H. Pu, and Y. Liu. 2010. Preparation of poly(3-hexylthiophene)/graphene nanocomposite via in situ reduction of modified graphite oxide sheets. *Appl. Surf. Science* 257:138–142.
- Yin, C., T. Kietzke, D. Neher, and H. Horhold. 2007. Photovoltaic properties and exciplex emission of polyphenylenevinylene-based blend solar cells. *Applied Physics Letters* 90:092117–092119.
- Yoshino, K., M. Onoda, Y. Manda, and M. Yokoyama. 1998. Electronic states in polythiophene and poly(3-methylthiophene) studied by photoelectron spectroscopy in air. *Japanese Journal of Applied Physics* 27(9):L1606–L1608.
- Yu, D., Y. Yang, M. Durstock, J. Baek, and L. Dai. 2010. Soluble P3HT-grafted graphene for efficient bilayer-heterojunction photovoltaic devices. *ACS Nano* 4(10):5633–5640.
- Yu, G., J. Gao, J. Hummelen, F. Wudl, and A. Heeger. 1995. Polymer photovoltaic cells: Enhanced efficiencies via a network of internal donor-acceptor heterojunctions. *Science* 270:1789–1791.
- Yu, Z., A. Raman, and S. Fan. 2010. Fundamental limit of nanophotonic light trapping in solar cells. Ginzton Laboratory, Stanford University, Stanford.
- Zhang, C., S. Tong, C. Jiang, E. Kang, D. Chan, and C. Zhu. 2008. Simple tandem organic photovoltaic cells for improved energy conversion efficiency. *Applied Physics Letters* 92:083310–083312.
- Zhang, F., W. Mammo, L. Andersson, S. Admassie, M. Andersson, and O. Inganäs. 2006. Low-bandgap alternating fluorine copolymer/methanofullerene heterojunctions in efficient near-infrared polymer solar cells. *Advanced Materials* 18(16):2169–2173.
- Zhao, J., J. Han, and J. Lu. 2002. Work functions of pristine and alkali-metal intercalated carbon nanotubes and bundles. *Physical Review B* 65:193401-1–193401-4.
- Zhao, J., A. Wang, and M. Green. 2001. High-efficiency PERL and PERT silicon solar cells on FZ and MCZ substrates. *Solar Energy Materials & Solar Cells* 65:429–435.
- Zhou, H., L. Yang, A. Stuart, S. Price, S. Liu, and W. You. 2011. Development of fluorinated benzothiadiazole as a structural unit for a polymer solar cell of 7% efficiency. *Angewandte Chemie International Edition* 50:2995–2998.